



Research paper

Time-Domain Analysis of Traveling Wave Switches Based on Time-Variant Transmission Line Model

H. Khoshniyat^{1,*}, G. Moradi², A. Abdipour²

¹Department of Electrical Engineering, Arak University of Technology, Arak, Iran.

²Department of Electrical Engineering, Amirkabir University of Technology, Tehran, Iran.

Article Info

Article History:

Received 04 June 2021

Reviewed 20 July 2021

Revised 11 October 2021

Accepted 16 October 2021

Keywords:

Finite-difference time-domain (FDTD) method

Fully-distributed model

Lossy transmission line model

Single Pole Single Throw (SPST)

Traveling wave switch (TWSW)

*Corresponding Author's Email Address:

Hkhoshniyat@arakut.ac.ir

Abstract

Background and Objectives: Switches play an important role in controlling the signal flow in telecommunication systems. The traveling wave switch structure is introduced based on active transmission lines. By applying the gate voltage (V_g), the transfer of signal through the drain transmission line is controlled. By increasing operating frequency, lumped model is unreliable and semi and fully distributed modeling should be applied for the analysis of these elements.

Methods: Traveling wave switches can be analyzed based on the lossy transmission line model, in linear and non-linear modes in the time and frequency domains. The study of transient behavior and time domain response of switch is very important. Switching and transient from on to off state and vice versa affect the performance of telecommunication systems. In the proposed method, the switch is modeled as the lossy transmission line that the primary elements of this model change with time based on the control voltage applied to the gate and are considered as variable with time. The structure is discretized in the space and time domains with Δz and Δt steps. The Finite-difference time-domain (FDTD) method is utilized to study the transient response of switches. By using the leap-frog algorithm, the new voltages and currents of the transmission line are calculated based on the values of adjacent spatial and temporal steps.

Results: The transient response of the switch is analyzed in transition from off to on states and vice versa, for the $800\mu\text{m}$ switch at 60GHz, based on the parameters of the passive transmission line and nonlinear Curtice2 FET model.

Conclusion: For transient analysis of the structure, the time-variant lossy transmission line model was used that its elements changed based on the applied control voltage. The results of FDTD method were investigated with the transient analysis of commercial software that showed good agreement with each other and hence validated the proposed method.

©2022 JECEI. All rights reserved.

Introduction

Nowadays, the request for millimeter-wave applications such as high-speed wireless LAN systems, radar systems is increasing quickly and also there is an enormous demand for microwave circuits to operate at higher and

higher frequencies to attain larger bandwidth. On the other hand, there has been an enlarged request for microwave integrated circuit application at higher frequencies caused by low fabrication cost and better operation at higher frequencies. Switches play an

important role in controlling the RF signal flow in transmitters and receivers of telecommunication and radar systems. In the mentioned applications, wideband switches with high power transfer capability and high switching speed, have an important duty in the implementation of low-cost communication systems. Due to the wide range of applications of millimeter wave circuits in high-speed communications and the important role of distributed switches in communication systems, much research has been done on various microwave switches to improve their performance. In this regard, some research has been done to improve parameters such as insertion loss and isolation. In millimeter-wave applications, various switch structures are reported in the literature [1]-[20].

The performance of a single-pole single-throw traveling-wave switch is analyzed with a lossy transmission line model in [1]. In [2], a single-pole double-throw traveling-wave switch using fully distributed FET has been developed and analyzed. [3] represents a switch structure that has a shunt structure in connection with a quarter wavelength transformer. The switches designed with this structure have an insertion loss less than 1.5 dB and isolation better than 25 dB in the frequency range from 59 GHz to 61 GHz. Another structure consists of a series FET in parallel with an inductor. Such a switch has an insertion loss of 1.6 dB and an isolation of 20 dB at 94 GHz [4]. In [5], another microwave switch with a parallel LC resonance structure, a capacitive stub and an inductor line, is indicated. A switch manufactured in this structure has an insertion loss of 3.9 dB and an isolation of 41 dB at 60 GHz. In [6], the series-shunt structures using the ohmic electrode sharing technology (OEST) have been introduced and discussed. Such a switch has an isolation of more than 20.6 dB and an insertion loss of less than 1.64 dB. In [7], a fast and flexible impedance matching technique is presented for MMIC switches based on the coupling matrix method by the field-effect-transistor-based (FET-based) resonator. By selecting appropriate coupling parameters, the MMIC switches can be easily designed without designing multistage impedance matching. [8] described the design of millimeter-wave wide-band monolithic GaAs passive high electron-mobility transistor (HEMT) switches using the traveling-wave concept. This type of switch combined the off-state shunt transistors and series microstrip lines to form an artificial transmission line with 50 Ω characteristic impedance. In [9] and [10], By using the fully distributed model and adjusting the switch length and operating frequency, various switch parameters such as insertion loss, isolation, and return loss are calculated. The optimum switch length and operating frequency are calculated versus the switch parameters especially the isolation and

the return loss in off and on conditions.

In [11], the design, analysis, and performance of four millimeter-wave SPDT switch MMICs are presented. The circuits utilize a 100-nm gate-length GaN-on-SiC technology and cover four different frequency ranges almost without a gap from 28 to 310 GHz. In [12], a single-pole single-throw switch monolithic microwave integrated circuit using 0.25 μm GaN HEMT technology is presented for Ka-band downlink frequencies 17 - 22 GHz. In [13], a structure of SPST switches was proposed to improve the return loss in off-state by applying quarter-wave transformers. The common SPST switches behave as a short or open circuit in off-state and reflect a high ratio of the signal. The semi-distributed and fully distributed analysis of the common and improved structure of SPST switches were shown improvement of matching in off state. In [14], a 36–38-GHz monolithic microwave integrated circuit (MMIC) single-pole double-throw (SPDT) switch employing a traveling-wave concept with absorptive characteristic is presented. The switch uses absorptive sections for better impedance matching in all ports.

In [15], A three-stage single pole single throw InGaAs pseudomorphic high electron mobility transistor monolithic microwave integrated circuit switch based on the HPF/LPF switching concept is introduced, with an insertion loss of less than 1.6 dB and isolation of more than 82 dB below 6 GHz, with a size of 1.1 mm \times 1.0 mm. In [16], to improve the return loss in the off state, a non-uniform structure of SPST switches is proposed which is based on the artificial tapered transmission line produced by applying various controlling voltage at the gate. In [17], high isolation K/Ka band monolithic microwave integrated circuit (MMIC) single pole double throw (SPDT) switches with shunt and series-shunt topologies were presented, by using a 70 nm GaAs HEMT process. In 24~27GHz, both switches demonstrated an isolation better than 39dB. The shunt type of switch demonstrated insertion loss less than 1.5dB and the series-shunt type of switch less than 2dB. [18] presented a low-loss and high Tx-to-Rx isolation single-pole double-throw (SPDT) millimeter-wave switch for true time delay applications. The switch was designed based on matching-network and double-shunt transistors with quarter-wavelength transmission lines. In [19], a low loss high isolation broadband single-port double-throw (SPDT) traveling-wave switch using 90 nm CMOS technology was presented. A body bias technique was utilized to enhance the circuit performance of the switch, especially for the operation frequency above 30 GHz. [20] presented a wideband digitally tunable SPST switch based on the travelling-wave concept that had been realized in a 22 nm FD-SOI CMOS technology. The digital control for return loss was performed through

mutual inductance switching. The proposed SPST switch achieves a bandwidth of 10-110 GHz, with an insertion loss of 1.2 dB at 60 GHz and a 24 dB isolation at 60 GHz.

Analysis of traveling-wave switches is done in the frequency domain, by considering the lossy transmission line model and scattering parameters. The use of ABCD transmission matrices and their conversion into scattering parameters is another common method in the frequency domain in non-uniform structures. Analysis of active transmission lines in the time domain is reported in linear and nonlinear regimes and the use of time-domain methods to analyze the transient behavior of the switch as an active transmission line is studied [21]-[25].

In this paper, the performance of traveling wave switches is investigated using the lossy transmission line model. For this purpose, the switch behavior is analyzed by using the finite difference time domain (FDTD) method and the structure is discretized in the space and time domains with Δz and Δt steps [25]. In this analysis, the switch is modeled as the lossy transmission line that the primary elements of this model change with time based on the control voltage applied to the gate and are considered as variable with time. With the help of this proposed method, instead of nonlinear analysis of the circuit, linear time-varying analysis can be used. The results obtained from this method are in good agreement with those of nonlinear analysis using commercial software. The switch performance is modelled well in the time domain in on, off and transient states.

Circuit Structure

The schematic of a Single-Pole Single-Throw (SPST) Traveling-Wave Switch (TWSW) is shown in Fig. 1 [1]. By applying the gate voltage (V_g), the transfer of signal through the drain transmission line is controlled. In this structure, the length of the switch is comparable to the wavelength of the maximum frequency of the circuit, so the wave transmission in this structure cannot be ignored and the lump model is unreliable and cannot analyze a distributed switch. Instead, distributed modeling should be applied for the analysis of these elements [2].

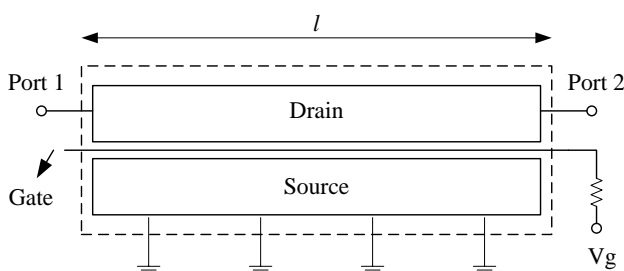


Fig. 1: Schematic of SPST traveling-wave switch [1].

In semi-distributed modeling, the device is sliced into N segments, that lumped modeling is reliable for each section.

If the number of slices approaches infinity, then the semi-distributed analysis turns to fully-distributed modeling. The sliced model of TWSW is shown in Fig. 2 [9].

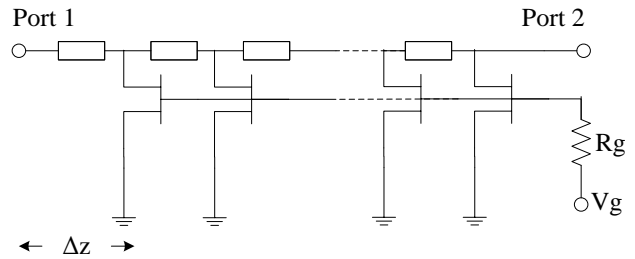


Fig. 2: Equivalent slice model of switch [9].

Fig. 3 shows the equivalent circuit seen from drain of transistor with Δz length. The values of nonlinear elements are obtained based on the Curtice model and with respect to the V_{gs} and V_{ds} voltages [21].

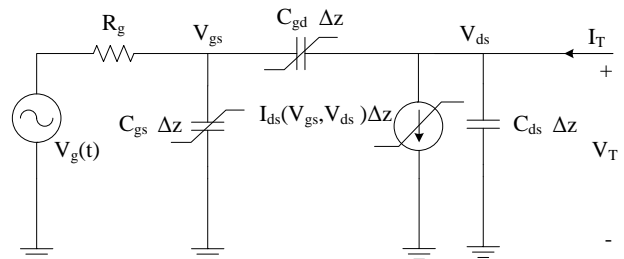


Fig. 3: The nonlinear equivalent circuit of a transistor with Δz length.

Due to the high input impedance of the gate and the low frequency of the control signal, the gate voltage can be considered equal to the control voltage with a good approximation. Also, assuming the amplitude of the input signal is small, the changes of C_{gd} and C_{gs} with V_{ds} are ignored and the nonlinear current source is modeled as G_{ds} conduction according to (1) and these values will be only a function of the control voltage. By considering the time variations of the control voltage $V_g(t)$, linear time-variant equivalent circuit of the transistor is obtained as shown in Fig. 4. The parameters C_{gs} , C_{gd} , C_{ds} and G_{ds} are defined per unit length of the transistor [10].

$$G_{ds}(t) = \left. \frac{\partial I_{ds}}{\partial V_{ds}} \right|_{V_{gs} = V_g(t)} \tag{1}$$

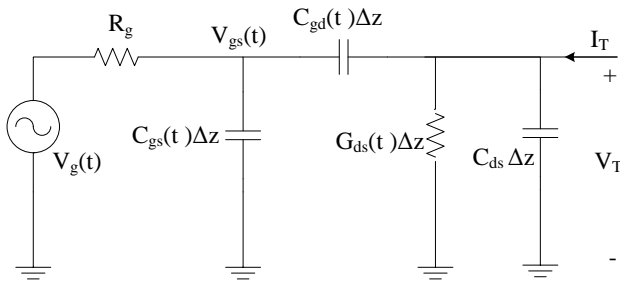


Fig. 4: The linear time-variant equivalent circuit of a transistor with Δz -length.

Using (2), the equivalent circuit seen from the drain of the transistor with length Δz can be considered as the summation of conductivity $G_{FET}(t)\Delta z$, capacitor $C_{FET}(t)\Delta z$ and current source $I_d(t)\Delta z$, which models the changes of control-voltage.

$$\begin{aligned}
 I_T &= C_{ds}\Delta z \frac{\partial V_T}{\partial t} + G_{ds}(t)\Delta z V_T + C_{gd}(t)\Delta z \frac{\partial}{\partial t}(V_T - V_g(t)) \\
 &= (C_{ds} + C_{gd}(t))\Delta z \frac{\partial V_T}{\partial t} + G_{ds}(t)\Delta z V_T - C_{gd}(t)\Delta z \frac{\partial V_g(t)}{\partial t} \quad (2) \\
 &= C_{FET}(t)\Delta z \frac{\partial V_T}{\partial t} + G_{FET}(t)\Delta z V_T + I_d(t)\Delta z
 \end{aligned}$$

Lossy Transmission Line Model

The lossy transmission line model of the switch is shown in Fig. 5. In this model, the elements $C(t)$, $G(t)$ and $I_d(t)$ of the transmission line change with time according to the control voltage applied to the gate of the transistor.

According to (3), $C(t)$ is obtained from the summation of the C_{TL} transmission line capacitor and the $C_{FET}(t)$ transistor capacitor [13].

$$C(t) = C_{TL} + C_{FET}(t) \quad (3)$$

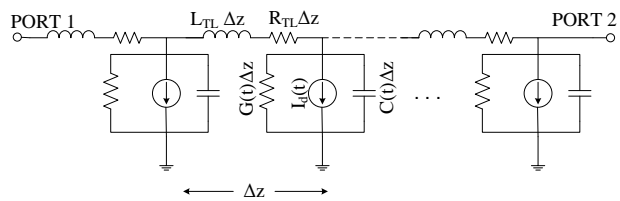


Fig. 5: Lossy transmission line model of TWSW.

The transmission line element with length Δz is shown in Fig. 6, using Kirchhoff's laws, the voltage and current relations for the differential element of the transmission line can be easily obtained. By tending Δz to zero and converting it to dz , the differential equations of the transmission line are obtained according to (4) and (5).

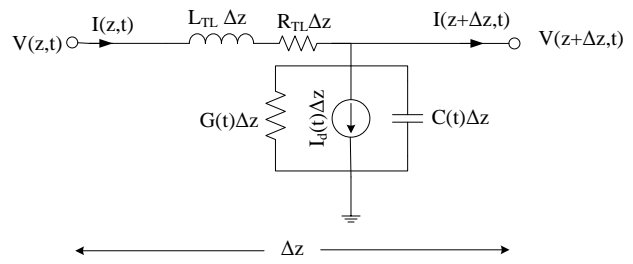


Fig. 6: Differential element of transmission line with length Δz .

$$\frac{dI(z,t)}{dz} + G(t)V(z,t) + C(t)\frac{dV(z,t)}{dt} + I_d(t) = 0 \quad (4)$$

$$\frac{dV(z,t)}{dz} + R_{TL}I(z,t) + L_{TL}\frac{dI(z,t)}{dt} = 0 \quad (5)$$

Analysis of Transmission Line Model by FDTD Method

The finite difference method is one of the common numerical methods in solving partial equations. This method is based on domain discretization to a set of nodes, approximation of differential equations with algebraic equations and solving algebraic equations based on the boundary and initial conditions. Using Taylor series is one of the methods of approximation of differential equations with algebraic equations.

In this method, the location axis is divided into Δz steps and the time axis is divided into Δt cells, which means that the z -axis is divided into Nz equal parts and the time axis is divided into Nt parts. Fig. 7 shows the discretization at the location axis and the voltage and current nodes for the transmission line model.

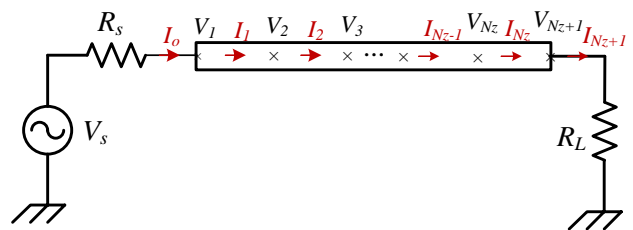


Fig. 7: Discretization of the transmission line model.

The method of voltage and current discretization is specified in (6) and (7). According to the method of discretization, $Nz + 1$ points of voltage and Nz points of current are located in z -direction. Fig. 8 shows the relationship between voltage and current at different points in two dimensions of time and space in the form of a graph for different time and space steps. In this method, the new value of the voltage at each point is calculated based on the amount of currents connected

to that node and the previous value of the voltage of that node.

The current is also updated based on the voltage of the adjacent nodes and the previous value of the current.

$$V_i^n \equiv V((i-1)\Delta z, n\Delta t) \tag{6}$$

$$I_i^n \equiv I((i-1/2)\Delta z, n\Delta t) \tag{7}$$

Using the backward difference approximation and Fig. 8, the differential equations of relations (4) and (5) become the algebraic form of relations (8) and (9) [25].

$$\frac{I_k^{n+1/2} - I_{k-1}^{n+1/2}}{\Delta z} + G^{n+1/2} \left(\frac{V_k^{n+1} + V_k^n}{2} \right) + \frac{C^{n+1/2}}{\Delta t} (V_k^{n+1} - V_k^n) + I_d^{n+1/2} = 0 \tag{8}$$

$$k = 2, 3, \dots, N_z$$

$$n = 0, 1, \dots, N_t$$

$$\frac{V_{k+1}^{n+1} - V_k^{n+1}}{\Delta z} + R_{TL} \left(\frac{I_k^{n+3/2} + I_k^{n+1/2}}{2} \right) + \frac{L_{TL}}{\Delta t} (I_k^{n+3/2} - I_k^{n+1/2}) = 0 \tag{9}$$

$$k = 1, 2, \dots, N_z$$

$$n = 0, 1, \dots, N_t$$

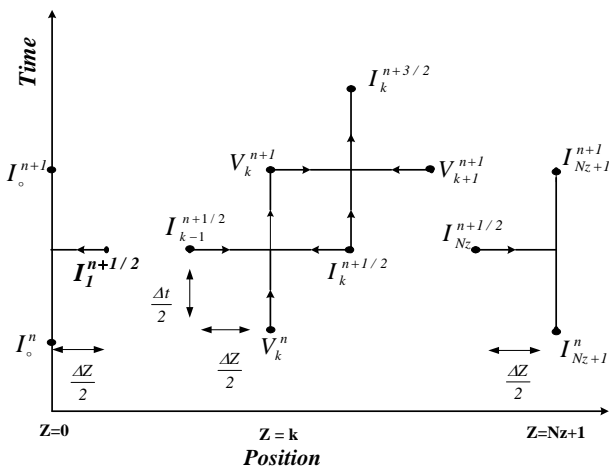


Fig. 8: The FDTD discretization of the voltage, current along the transmission line [25].

By arranging the (8) and (9), the expression of V_k^{n+1} and $I_k^{n+3/2}$ can be extracted and (10) and (11) are obtained.

$$\left(\frac{C^{n+1/2}}{\Delta t} + \frac{G^{n+1/2}}{2} \right) V_k^{n+1} = \left(\frac{C^{n+1/2}}{\Delta t} - \frac{G^{n+1/2}}{2} \right) V_k^n + \frac{I_{k-1}^{n+1/2} - I_k^{n+1/2}}{\Delta z} - I_d^{n+1/2} \tag{10}$$

$$k = 2, 3, \dots, N_z$$

$$n = 0, 1, \dots, N_t$$

$$\left(\frac{L_{TL}}{\Delta t} + \frac{R_{TL}}{2} \right) I_k^{n+3/2} = \left(\frac{L_{TL}}{\Delta t} - \frac{R_{TL}}{2} \right) I_k^{n+1/2} + \frac{V_k^{n+1} - V_{k+1}^{n+1}}{\Delta z} \tag{11}$$

$$k = 1, 2, \dots, N_z$$

$$n = 0, 1, \dots, N_t$$

By simplifying relations (10) and (11), relations (12) and (13) are obtained.

These relations are used to obtain new values of I_k and V_k , matrices A, B, E and F are introduced in relations (14) and (15) [25].

$$V_k^{n+1} = A \cdot B \cdot V_k^n + \frac{A}{\Delta z} (I_{k-1}^{n+1/2} - I_k^{n+1/2} - \Delta z I_d^{n+1/2}) \tag{12}$$

$$k = 2, 3, \dots, N_z$$

$$n = 0, 1, \dots, N_t$$

$$I_k^{n+3/2} = E \cdot F \cdot I_k^{n+1/2} + \frac{E}{\Delta z} (V_k^{n+1} - V_{k+1}^{n+1}) \tag{13}$$

$$k = 1, 2, \dots, N_z$$

$$n = 0, 1, \dots, N_t$$

$$A = \left(\frac{C^{n+1/2}}{\Delta t} + \frac{G^{n+1/2}}{2} \right)^{-1}, B = \left(\frac{C^{n+1/2}}{\Delta t} - \frac{G^{n+1/2}}{2} \right) \tag{14}$$

$$E = \left(\frac{L_{TL}}{\Delta t} + \frac{R_{TL}}{2} \right)^{-1}, F = \left(\frac{L_{TL}}{\Delta t} - \frac{R_{TL}}{2} \right) \tag{15}$$

It is also necessary to consider the boundary conditions at the beginning and end of the line to solve the problem and find the voltages V_1 and V_{Nz+1} the source and load currents are considered I_0 and I_{Nz+1} , respectively and (8) for the values $k = 1$ and $k = Nz + 1$ is modified as:

$$k = 1 \Rightarrow \frac{1}{\Delta z} \left(I_1^{n+1/2} - \frac{I_0^{n+1} + I_0^n}{2} \right) + \frac{C^{n+1/2}}{\Delta t} (V_1^{n+1} - V_1^n) + \frac{G^{n+1/2}}{2} (V_1^{n+1} + V_1^n) + I_d^{n+1/2} = 0 \tag{16}$$

$$k = N_z + 1 \Rightarrow \frac{1}{\Delta z} \left(\frac{I_{Nz+1}^{n+1} + I_{Nz+1}^n}{2} - I_{Nz}^{n+1/2} \right) + \frac{C^{n+1/2}}{\Delta t} (V_{Nz+1}^{n+1} - V_{Nz+1}^n) + \frac{G^{n+1/2}}{2} (V_{Nz+1}^{n+1} + V_{Nz+1}^n) + I_d^{n+1/2} = 0 \tag{17}$$

The distance between the current I_1 and the source current is equal to $\Delta z/2$, for this reason in (16) which describes the boundary condition of the source, the coefficient of the current term at the denominator is

considered to be $\Delta z/2$ instead of Δz . The same operation is repeated for the boundary condition of the load terminal. The relations (16) and (17) are transformed as:

$$V_1^{n+1} = ABV_1^n + \frac{2A}{\Delta z} \left(I_o^{n+1/2} - I_1^{n+1/2} - \frac{\Delta z}{2} I_d^{n+1/2} \right) \quad (18)$$

$$n = 0, 1, \dots, N_t$$

$$V_{N_z+1}^{n+1} = ABV_{N_z+1}^n + \frac{2A}{\Delta z} \left(I_{N_z}^{n+1/2} - I_{N_z+1}^{n+1/2} - \frac{\Delta z}{2} I_d^{n+1/2} \right) \quad (19)$$

$$n = 0, 1, \dots, N_t$$

According to Fig. 9 and the series resistor at the beginning and end of the line, the current relationships can be achieved simply, by applying the KCL equations in these two nodes that are expressed in (20) and (21) [25].

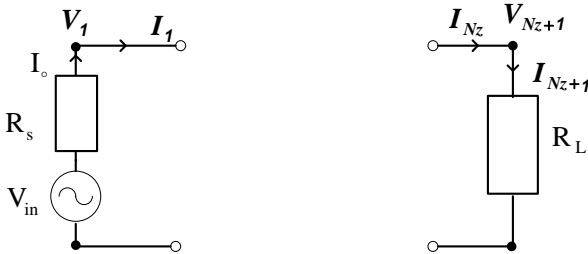


Fig. 9: Source and load currents at input and output nodes [25].

$$I_o^{n+1/2} = \frac{V_{in}^n + V_{in}^{n+1} - V_1^n - V_1^{n+1}}{2R_s} \quad (20)$$

$$I_{N_z+1}^{n+1/2} = \frac{V_{N_z+1}^n + V_{N_z+1}^{n+1}}{2R_L} \quad (21)$$

Finally, the obtained equations are arranged and the set of recursive equations is obtained, which express the voltage and current at different points of the line and at different times. These equations are expressed in (22) to (25).

$$V_1^{n+1} = \left(AB - \frac{A}{\Delta z R_s} \right) \left(1 + \frac{A}{\Delta z R_s} \right)^{-1} V_1^n + \frac{2A}{\Delta z} \times \left(1 + \frac{A}{\Delta z R_s} \right)^{-1} \left(\frac{V_{in}^{n+1} + V_{in}^n}{2R_s} - I_1^{n+1/2} - \frac{\Delta z}{2} I_d^{n+1/2} \right) \quad (22)$$

$$V_k^{n+1} = A.B.V_k^n + \frac{A}{\Delta z} \left(I_{k-1}^{n+1/2} - I_k^{n+1/2} - \Delta z I_d^{n+1/2} \right) \quad (23)$$

$$k = 2, 3, \dots, N_z$$

$$V_{N_z+1}^{n+1} = \left(AB - \frac{A}{\Delta z R_L} \right) \left(1 + \frac{A}{\Delta z R_L} \right)^{-1} V_{N_z+1}^n + \frac{2A}{\Delta z} \left(1 + \frac{A}{\Delta z R_L} \right)^{-1} \left(I_{N_z}^{n+1/2} - \frac{\Delta z}{2} I_d^{n+1/2} \right) \quad (24)$$

$$I_k^{n+3/2} = E.F.I_k^{n+1/2} + \frac{E}{\Delta z} (V_k^{n+1} - V_{k+1}^n) \quad (25)$$

$$k = 1, 2, \dots, N_z$$

First, the voltage of the first node is obtained by (22), the initial voltages and currents of the transmission line are assumed zero. In the next step, for $k = 2, 3, \dots, N_z$ and by (23), the voltages of the other nodes are obtained according to the voltages and currents in the previous step. The voltage of the last node is calculated using (24) for $k = N_z + 1$ and the values of voltage and current in the previous time step. After calculating the voltages in the new time step, the currents of the nodes in the new time step are calculated using (25) by the voltages and currents of the nodes in the previous step. This process will continue until reach the last time step. This algorithm is known as the leap-frog algorithm. This flowchart is shown in Fig. 10.

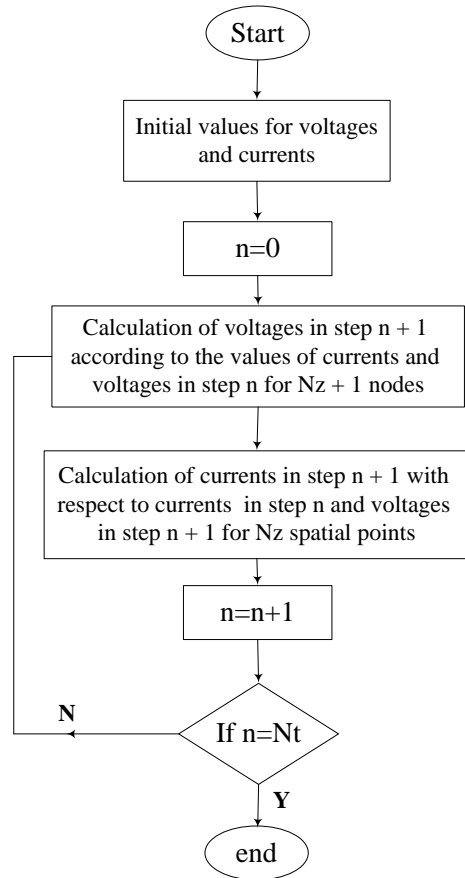


Fig. 10: Flowchart of the leap-frog algorithm for solving transmission line equations.

The structure of a traveling-wave switch similar to a FET transistor consists of active and passive parts. The passive part represents the attenuation and coupling of transmission lines and its elements are shown in Table 1.

Table 1: Numerical values of the passive transmission line model

Parameter	Value
L_{TL}	400 nH/m.
R_{TL}	900 ohm/m
C_{TL}	70 pF/m

The Curtice2 model is used to analyze the active part of the switch. In this model, the nonlinear current source (I_{ds}) is defined according to voltages of the transistor (26), knowing that if the V_{gs} is smaller than V_{T0} then the current source is zero. In this equation, α , β and λ are fixed parameters of the model and V_{T0} is the pinch-off voltage of the transistor. The term $(V_{gs} - V_{T0})^2$ illustrates I_{ds} with respect to V_{gs} as a quadratic polynomial and this is why this model is named Curtice2. The nonlinear gate-source and gate-drain capacitances are described in the Curtice2 as (27), (28). C_{gs0} and C_{gd0} are the zero-bias gate and drain capacitances, respectively, and V_{bi} the built-in gate potential. The elements of this section are obtained by scaling from the parameters of the 100 μm transistor model that are shown in Table 2.

$$I_{ds}(V_{gs}, V_{ds}) = \beta(V_{gs} - V_{T0})^2 (1 + \lambda V_{ds}) \tanh(\alpha V_{ds}) \quad (26)$$

$$C_{gs} = C_{gs0} \times \left(1 - \frac{V_{gs}}{V_{bi}}\right)^{-1/2} \quad (27)$$

$$C_{gd} = C_{gd0} \times \left(1 - \frac{V_{gd}}{V_{bi}}\right)^{-1/2} \quad (28)$$

Table 2: Curtice2 model's parameters for 100 μm FET

Parameter	Value
β	0.0162 A/V ²
α	1.3 V ⁻¹
λ	0 V ⁻¹
V_{T0}	-2.35 V
C_{gs0}	12 fF
C_{gd0}	5.915 fF
C_{ds}	17.745 fF
V_{bi}	0.85 V

The study of transient behavior and time domain response of switch is very important. Switching and

transient from on to off state and vice versa affect the performance of telecommunication systems. In this section, the analysis results of the 800 μm switch with the time-varying transmission line model in the time domain are presented and compared with the results of the nonlinear analysis of commercial software.

According to the initial parameters of the switch and considering the maximum frequency of 500 GHz, the division into 80 parts is sufficient for the 800 μm structure and the assumption of the lumped element is valid for 10 μm segments. To study the performance of the switch, a 10 mV signal with 60 GHz frequency has been applied to the drain transmission line. A pulse-shaped control signal with a period of 20 nsec and rise and fall time of 1 nsec has been used to on and off the switch as well. The control voltage has the low and high levels of -5 V and 0 V respectively, that the transistor was on at low voltage and was in the cut-off mode at high voltage. The variation of control voltage from low to high level and vice versa has the cosine form. By applying the RF signal and the control voltage Vg with the mentioned parameters, the switch behavior in the transition mode from on to off state and vice versa is shown in Fig. 11 and Fig. 12. In these figures, the performance of the switch is analyzed by the linear time-varying model method and the nonlinear method, which have good agreement. In the linear time-varying method, as mentioned, the transmission line parameters change with time. These results are calculated with Matlab by applying the FDTD method to the 800 μm switch that is divided into 80 segments. In the nonlinear method, quasi-distributed analysis of the switch was performed by commercial software. In Fig. 11, which shows the behavior of the switch in the transition from off to on state, by passing the control voltage through the threshold voltage V_{T0} , the performance of the switch changes and the RF signal is transmitted by the switch. Due to the small amplitude of the information signal, in the transition mode due to changes in the control voltage, which is modeled as the current source, a downward jump is observed in the output of the switch.

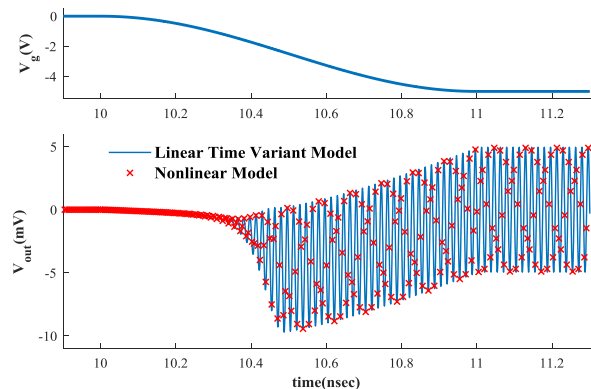


Fig. 11: Transient of 800 μm TWSW from off to on mode.

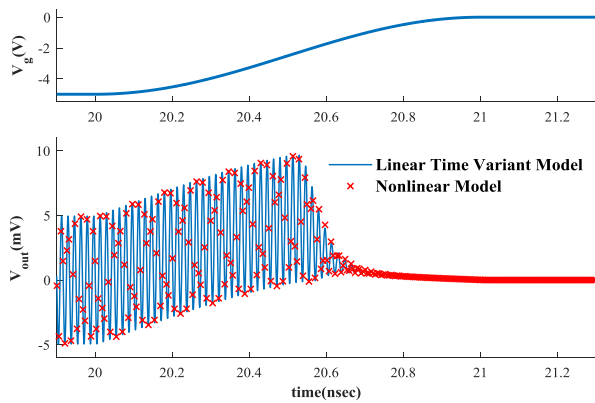


Fig. 12: Transient of 800 μm TWSW from on to off mode.

Fig. 12 shows the operation of the switch in the transition from on to off state. Same as the previous figure, when the control voltage passes through the threshold voltage V_{T0} , the status of the switch changes and the passage of the information signal by the switch stops. In this case, the output signal jumps upwards.

This jump can be considered as a zero input response that is added to the input response. In this case, if the input range is large, this jump is small compared to it and is not sensed at the output. If the amplitude of the input signal is small, the jumps have an amplitude several times the information signal at the output, which may damage or saturate the next blocks. Therefore, in small-signal applications, the amplitude of these jumps should be reduced, for example, by reducing the difference in the level of the control signal or increasing its rise time and fall time, the temporal changes of the control signal were slower and fewer jumps are felt at the output.

Conclusion

The switch has a major role in the realization of communication systems and analysis of their performance is very important. Traveling-wave switches can be analyzed based on the lossy transmission line model, in linear and non-linear modes in the time and frequency domains. Comparison between the analysis methods is illustrated in Table 3. Time domain and transient analysis of the switch were studied to investigate its behavior during the transition from on to off state and vice versa and the possibility of an overshoot in the output signal that may cause damage to other parts of the system that necessitates transient analysis. For transient analysis of the structure, the time-variant lossy transmission line model was used that its elements were changed based on the applied control voltage. The results of the FDTD method were investigated with the transient analysis of a commercial software that showed good agreement with each other and hence validated the proposed method.

Table 3: Comparison between the analysis methods

Ref.	Details (Methods/linear or nonlinear/ frequency or time domains)
[1], [2]	S-parameters from lossy transmission line model, linear, frequency domain analysis.
[7]	Analytical design of switches using FET-based resonators and coupling matrix method, S-parameters frequency domain.
[8], [12], [13], [14], [19], [20]	S-parameters by using the ABCD matrix, linear, frequency domain analysis.
[9], [10]	Semi and fully-distributed analysis, linear S-parameters frequency domain.
[15]	MMIC SPST switch based on HPF/LPF switching concept, linear S-parameters frequency domain.
[22], [23]	FDTD Analysis of Small Signal Model for Active Multi-conductor Transmission Line (AMTL), time domain.
[25]	Nonlinear and fully distributed modelling of Nonlinear Active Multi-conductor Transmission Line (NAMTL) using time-domain. method
This work	FDTD analysis based on time-variant transmission line model, transient analysis.

Author Contributions

H. Khoshniyat proposed a model and did the simulations. H. Khoshniyat, G. Moradi and A. Abdipour interpreted the results and wrote the manuscript.

Conflict of Interest

The author declares that there is no conflict of interests regarding the publication of this manuscript. In addition, the ethical issues, including plagiarism, informed consent, misconduct, data fabrication and/or falsification, double publication and/or submission, and redundancy have been completely observed by the authors.

Abbreviations

AMTL	Active Multiconductor Transmission Line
FDTD	Finite-difference time-domain
NAMTL	Nonlinear Active Multiconductor Transmission Line
SPDT	Single Pole Double Throw
SPST	Single Pole Single Throw

TL	Transmission line
TWSW	Traveling wave switch

References

- [1] H. Mizutani, Y. Takayama, "DC-110-GHz MMIC traveling wave switch," *IEEE Trans. Microwave Theory Tech.*, 48(5): 840-845, 2000.
- [2] H. Mizutani, N. Iwata, Y. Takayama, K. Honjo, "Design considerations for traveling-wave single-pole multi throw MMIC switch using fully distributed FET," *IEEE Trans. Microwave Theory Tech.*, 55(4): 664-671, 2007.
- [3] G.L. Lan, D.L. Dunn, J.C. Chen, C.K. Pao, D.C. Wang, "A high performance V-band monolithic FET transmit-receive switch," in *Proc. IEEE Microwave Millimeter-Wave Monolithic Circuits Symposium*: 99-101, 1988.
- [4] H. Takasu, F. Sasaki, H. Kawasaki, H. Tokuda, S. Kamihashi, "W-band SPST transistor switches," *IEEE Microwave Guided Wave Lett.*, 6: 315-316, 1996.
- [5] M. Madhian, L. Desclos, K. Maruhashi, K. Onda, M. Kuzuhara, "A high-speed resonance-type FET transceiver switch for millimeter-wave band wireless networks," in *Proc. 26th European Microwave Conference*: 941-944, 1996.
- [6] H. Mizutani, M. Funabashi, M. Kuzuhara, Y. Takayama, "Compact DC-60 GHz HJFET MMIC switches using ohmic electrode-sharing technology," *IEEE Trans. Microwave Theory Tech.*, 46: 1597-1603, 1998.
- [7] G. Shen, W. Che, H. Zhu, F. Xu, Q. Xue, "Analytical design of millimeter-wave 100-nm GaN-on-Si MMIC switches using FET-based resonators and coupling matrix method," *IEEE Trans. Microwave Theory Tech.*, 69(7): 3307-3318, 2021.
- [8] K. - Lin, Wen-Hua Tu, Ping-Yu Chen, Hong-Yeh Chang, Huei Wang, Ruey-Beei Wu, "Millimeter-wave MMIC passive HEMT switches using traveling-wave concept," *IEEE Trans. Microwave Theory Tech.*, 52(8): 1798-1808, 2004.
- [9] H. Khoshniyat, G. Moradi, A. Abdipour, K. Afrooz, "Optimization and fully distributed analysis of traveling wave switches at millimeter wave frequency band," in *Proc. 1st MMWATT Conference*: 45-49, 2009.
- [10] H. Khoshniyat, G. Moradi, A. Abdipour, K. Afrooz, "Optimization and fully-distributed analysis of single-pole single-throw traveling wave switches at millimeter wave frequency band," *Int. J. Inf. Commun. Technol. (IJICT)*, 3(2): 19-25, 2011.
- [11] F. Thome, P. Brückner, R. Quay, O. Ambacher, "Millimeter-wave single-pole double-throw switches based on a 100-nm gate-length AlGaIn/GaN-HEMT technology," in *Proc. 2019 IEEE MTT-S International Microwave Symposium (IMS)*: 1403-1406, 2019.
- [12] S. Kaleem, J. Kühn, R. Quay, M. Hein, "A high-power Ka-band single-pole single-throw switch MMIC using 0.25 μm GaN on SiC," in *Proc. 2015 IEEE Radio and Wireless Symposium (RWS)*: 132-134, 2015.
- [13] H. Khoshniyat, G. Moradi, A. Abdipour, K. Afrooz, "Fully distributed analysis of an improved single pole single throw traveling wave switches," in *Proc. 21st Iranian Conference on Electrical Engineering (ICEE 2013)*: 1-4, 2013.
- [14] K.T. Trinh, H. Kao, H. Chiu, N.C. Karmakar, "A Ka-Band GaAs MMIC traveling-wave switch with absorptive characteristic," *IEEE Microwave and Wireless Compon. Lett.*, 29(6): 394-396, 2019.
- [15] H. Mizutani, R. Ishikawa, K. Honjo, "InGaAs MMIC SPST switch based on HPF/LPF switching concept with periodic structure," *IEEE Trans. Microwave Theory Tech.*, 64(9): 2863-2870, 2016.
- [16] H. Khoshniyat, A. Abdipour, G. Moradi, "Fully distributed modeling, analysis and simulation of an improved non-uniform traveling wave structure," *AUT J. Model. Simul.*, 46: 47-52, 2014.
- [17] L. Zhang, X. Cheng, X. Deng, X. Li, "Design of K/Ka-band passive HEMT SPDT switches with high isolation," in *Proc. 2017 China Semiconductor Technology International Conference (CSTIC)*: 1-3, 2017.
- [18] C.W. Byeon, C.S. Park, "Design and analysis of the millimeter-wave SPDT switch for TDD applications," *IEEE Trans. Microwave Theory Tech.*, 61(8): 2858-2864, 2013.
- [19] H. Chang, C. Chan, "A low loss high isolation DC-60 GHz SPDT traveling-wave switch with a body bias technique in 90 nm CMOS process," *IEEE Microwave Wireless Compon. Lett.*, 20(2): 82-84, 2010.
- [20] R. Ciocoveanu, R. Weigel, A. Hagelauer, V. Issakov, "A low insertion-loss 10–110 GHz digitally tunable SPST switch in 22 nm FD-SOI CMOS," in *Proc. 2018 IEEE BiCMOS and Compound Semiconductor Integrated Circuits and Technology Symposium (BCICTS)*: 1-4, 2018.
- [21] W.R. Curtice, "A MESFET for use in design of GaAs ICs," *IEEE Trans. on Microwave Theory Tech.*, MTT-28: 448-456, 1980.
- [22] K. Afrooz, A. Abdipour, A. Tavakoli, M. Movahhedi, "FDTD analysis of small signal model for GaAs MESFETs based on three line structure," in *Proc. 2007 Asia-Pacific Microwave Conference*: 1-4, 2007.
- [23] F. Daneshmandian, A. Abdipour, R. Mirzavand, "A three-conductor transmission line model for MOS transistors," *Appl. Comput. Electromagn. Soc. (ACES)*, 30(6): 670-676, 2015.
- [24] C.R. Paul, *Analysis of Multiconductor Transmission Lines*, 2nd edition, John Wiley & Sons, Inc., Hoboken, New Jersey, 2008.
- [25] K. Afrooz, A. Abdipour, A. Tavakoli, M. Movahhedi, "Nonlinear and fully distributed field effect transistor modelling procedure using time-domain method," *IET Microwaves Antennas Propag.*, 2(8): 886-897, 2008.

Biographies



passive microwave devices and circuits and microwave measurement.

Hamed Khoshniyat was born in Karaj, Iran, in 1985. He received B.Sc., M.Sc. and Ph.D. degrees from Amirkabir University of Technology (Tehran Polytechnic), Tehran, Iran, all in electrical engineering, in 2008, 2010 and 2017 respectively. He is currently an Assistant Professor with the Electrical Engineering Department, Arak University of Technology. His current research interests include analysis and modeling of distributed amplifiers and switches, non-Foster elements, active and



February 2017. He is currently an Associate Professor with the Electrical Engineering Department, Amirkabir University of Technology. He has published or presented more than 100 articles in refereed journals and international conferences.

Gholamreza Moradi was born in Shahriar, Iran, in 1966. He received the B.Sc. degree from Tehran University, the M.Sc. degree from IUST, and the Ph.D. degree from Tehran Polytechnic, all in electrical engineering. His main research interests are numerical electromagnetics, antennas, passive and active microwave, and mm-wave circuits and systems. He has served as a Visiting Professor with the University of Alberta, from June 2016 until



Abdolali Abdipour was born in Alashtar, Iran, in 1966. He received the B.Sc. degree in electrical engineering from Tehran University, Tehran, Iran, in 1989, the M.Sc. degree in electronics from Limoges University, Limoges, France, in 1992, and the Ph.D. degree in electronic engineering from Paris XI University, Paris, France, in 1996. He is currently a Professor in the Electrical Engineering Department, Amirkabir University of Technology (Tehran Polytechnic), Tehran.

He has authored five books, Noise in Electronic Communication: Modeling, Analysis and Measurement (Amirkabir University Press,

2005, in Persian), Transmission Lines (Nahre Danesh Press, 2006, in Persian), Active Transmission Lines in Electronics and Communications: Modeling and Analysis (Amirkabir University Press, 2007, in Persian top selected book of the year), Communication Circuits (Nonlinear Analysis, Design and Simulation (Nass Press, 2013), and High-Frequency Field Effect Transistors (Electronic electromagnetics Modeling analysis, Amirkabir University Press, 2013, in Persian). He has authored or coauthored more than 330 articles in refereed journals and local and international conferences. His research areas include wireless communication systems (RF technology and transceivers), RF/microwave/millimeter-wave/THz circuit and system design, electromagnetic (EM) modeling of active devices and circuits, high-frequency electronics (signal and noise), nonlinear modeling, and analysis of microwave devices and circuits.

Copyrights

©2022 The author(s). This is an open access article distributed under the terms of the Creative Commons Attribution (CC BY 4.0), which permits unrestricted use, distribution, and reproduction in any medium, as long as the original authors and source are cited. No permission is required from the authors or the publishers.



How to cite this paper:

H. Khoshniyat, G. Moradi, A. Abdipour, "Time-domain analysis of traveling wave switches based on time-variant transmission line model," J. Electr. Comput. Eng. Innovations, 10(1): 221-230, 2022.

DOI: [10.22061/JECEI.2021.8126.483](https://doi.org/10.22061/JECEI.2021.8126.483)

URL: https://jecei.sru.ac.ir/article_1610.html

